

# On the possibility to search for $2\beta$ decay of initially unstable ( $\alpha/\beta$ radioactive) nuclei

V.I. Tretyak, F.A. Danevich, S.S. Nagorny, Yu.G. Zdesenko

*Institute for Nuclear Research, MSP 03680 Kiev, Ukraine*

## Abstract

Possibilities to search for  $2\beta$  decay of  $\alpha/\beta$  unstable nuclei, many of which have higher energy release than “conventional” ( $\beta$  stable)  $2\beta$  candidates, are discussed. First experimental half-life limits on  $2\beta$  decay of radioactive nuclides from U and Th families (trace contaminants of the  $\text{CaWO}_4$ ,  $\text{CdWO}_4$  and  $\text{Gd}_2\text{SiO}_5$  scintillators) were established by reanalyzing the data of low-background measurements in the Solotvina Underground Laboratory with these detectors (1734 h with  $\text{CaWO}_4$ , 13316 h with  $\text{CdWO}_4$ , and 13949 h with  $\text{Gd}_2\text{SiO}_5$  crystals).

PACS numbers: 23.40.-s; 23.60.+e; 27.70.+q; 27.80.+w; 27.90.+b; 29.40.Mc

Keywords: double  $\beta$  decay,  $^{232}\text{Th}$ ,  $^{238}\text{U}$ ,  $\text{CaWO}_4$ ,  $\text{CdWO}_4$  and  $\text{Gd}_2\text{SiO}_5$  crystal scintillators

## 1 Introduction

Recent observations of neutrino oscillations with atmospheric [1], solar [2], reactor [3] and accelerator [4] neutrinos manifest the non-zero neutrino mass and prove an existence of new physical effects beyond the Standard Model (SM) of electroweak theory. The discovery of the neutrino mass gives an extraordinary motivation for experimental searches for neutrinoless ( $0\nu$ ) double beta ( $2\beta$ ) decay of atomic nuclei, an exotic process (forbidden in the SM), which violates the lepton number on two units [5, 6, 7]. While oscillation experiments are sensitive only to the neutrino mass difference, the measured  $0\nu 2\beta$  decay rate can give an absolute scale of the effective Majorana neutrino mass and, consequently, could test different neutrino mixing models.

Up-to-date this process still remains unobserved, and only half-life limits for  $0\nu$  mode were established in direct experiments (see reviews [5, 6, 7] and compilation of  $2\beta$  decay results [8]). The highest bounds were obtained for the following nuclides:  $T_{1/2}^{0\nu} \geq 10^{21}$  yr for  $^{48}\text{Ca}$  [9],  $^{150}\text{Nd}$  [10],  $^{160}\text{Gd}$  [11],  $^{186}\text{W}$  [12];  $T_{1/2}^{0\nu} \geq 10^{22}$  yr for  $^{82}\text{Se}$  [13],  $^{100}\text{Mo}$  [14];  $T_{1/2}^{0\nu} \geq 10^{23}$  yr for  $^{116}\text{Cd}$  [15],  $^{128}\text{Te}$ ,  $^{130}\text{Te}$  [16],  $^{136}\text{Xe}$  [17]; and  $T_{1/2}^{0\nu} \geq 10^{25}$  yr for  $^{76}\text{Ge}$  [18]. These results have already brought the most stringent restrictions on the values of the Majorana neutrino mass  $\langle m_\nu \rangle \leq 0.2\text{--}2$  eV, the right-handed admixtures in the weak interaction  $\eta \approx 10^{-8}$ ,  $\lambda \approx 10^{-6}$ , the neutrino-Majoron coupling constant  $g_M \approx 10^{-4}$ , and the  $R$ -parity violating parameter of minimal supersymmetric standard model  $\approx 10^{-4}$  [5, 6, 7, 8].

However, to make the *discovery* of the  $0\nu 2\beta$  decay indeed realistic, the present level of the experimental sensitivity should be enhanced to  $\langle m_\nu \rangle \approx 0.01$  eV. It is the great challenge, and

several large-scale projects of the next generation experiments on  $0\nu 2\beta$  decay search were proposed during few last years, like CAMEO, EXO, GEM, GENIUS, Majorana, MOON and others (see, f.e., reviews [5, 6, 7]). These projects intend to use up to tons of super-low background detectors made of enriched  $2\beta$  isotopes, and plan to perform measurements with them during at least  $\approx 10$  years. However, there is a chance that even for so ambitious projects the required advancement of the experimental sensitivity could be not reached in virtue of the restrictions of the current technologies. Therefore, investigation of other nonstandard approaches and discussion of some new and even unusual ideas could be fruitful for the future of the  $2\beta$  decay research.

In the process of  $2\beta^-$  (or  $2\beta^+$ ) decay (see Fig. 1a) two electrons (or positrons) are emitted simultaneously, thus, an initial nucleus  $(A, Z)$  is transformed to  $(A, Z+2)$  or to  $(A, Z-2)$ , which is, in principle, possible if mass of initial nucleus  $M(A, Z)$  is larger than mass of final nucleus  $M(A, Z \pm 2)$ . Nevertheless, quite often, to surprise, the statement can be found in a literature that  $2\beta$  decay can occur in only case if: (a)  $M(A, Z) > M(A, Z \pm 2)$ ; (b) ordinary  $\beta$  decay of the initial nucleus  $(A, Z)$  to the intermediate nucleus  $(A, Z \pm 1)$  is forbidden energetically (that is  $M(A, Z) < M(A, Z \pm 1)$ ), or such a  $\beta$  decay  $(A, Z) \rightarrow (A, Z \pm 1)$  is suppressed by a large difference in spin between parent  $(A, Z)$  and intermediate  $(A, Z \pm 1)$  nuclei. However, it is clear that demand (b) is not mandatory – in fact, it just specifies conditions, which makes  $2\beta$  decay study convenient, because in the case of a  $\beta$  unstable parent nucleus, it would be extremely difficult to distinguish  $2\beta$  decays from the intensive  $\beta$  background. To this effect, until now only “conventional”  $2\beta$  decay candidate nuclei, satisfying both demands (a) and (b), were studied in direct experiments [5, 6, 7, 8].

However, investigation of the  $2\beta$  decay of initially unstable ( $\beta$  or/and  $\alpha$ ) nuclei (see Fig. 1b, 1c), despite its complications, could be interesting too [8]. With this aim, let us consider formula for the  $0\nu 2\beta$  decay probability, restricting to the neutrino mass mechanism only (right-handed contributions are neglected) [19]:  $(T_{1/2}^{0\nu})^{-1} = F^{0\nu} \cdot |\text{NME}|^2 \cdot \langle m_\nu \rangle^2$ . Here,  $F^{0\nu}$  is the phase space factor (proportional to the fifth power of energy release in  $2\beta$  decay,  $Q_{\beta\beta}$ ), and NME is the corresponding nuclear matrix element. Thus, the bound on the effective neutrino mass,  $\langle m_\nu \rangle$ , which could be derived from the experimental half-life limit,  $T_{1/2}^{exp}$ , can be expressed as follows:  $\lim \langle m_\nu \rangle \sim |\text{NME}|^{-1} \cdot \{Q_{\beta\beta}^5 \cdot T_{1/2}^{exp}\}^{-1/2}$ . Last equation means that sensitivity of  $2\beta$  experiment to the neutrino mass bound (for the equal NME and  $T_{1/2}^{exp}$  limit) is proportional to the  $Q_{\beta\beta}^{-5/2}$ , hence, the larger  $Q_{\beta\beta}$  value, the more stringent  $\langle m_\nu \rangle$  restriction could be derived. For any of 69 “conventional”  $2\beta^\pm$  decay candidate nuclei [8] this  $2\beta$  energy release does not exceed  $\approx 4.3$  MeV,<sup>1</sup> while for some  $2\beta^\pm$  nuclides, not satisfying demand (b), the  $Q_{\beta\beta}$  values are up to ten times larger [20]. The energy releases [20] for all possible  $2\beta^\pm$  candidates ( $\simeq 2300$ ) are shown in Fig. 2 in comparison with those available for “conventional”  $2\beta$  nuclides.<sup>2</sup> For example,  $Q_{\beta\beta}$  for  $^{19}\text{B}$  (or  $^{22}\text{C}$ ) is equal  $\approx 43$  MeV, therefore its  $0\nu 2\beta$  decay rate would be  $\approx 4 \times 10^6$  times faster than that for  $^{76}\text{Ge}$  with  $Q_{\beta\beta} \approx 2$  MeV (supposing equal NME-s).

Obviously, because of very hard problem in accumulating a large amount of fast-decaying parent nuclei, and due to enormous difficulties in discrimination of  $2\beta$  decay events from intensive  $\beta$  background, no schemes of  $2\beta$  experiments involving “unconventional” candidates have

<sup>1</sup>In fact, 2 nuclides from that list,  $^{48}\text{Ca}$  and  $^{96}\text{Zr}$ , are potentially  $\beta$  decaying, however, up-to-date their  $\beta$  decays were not observed being strongly suppressed because of a large change in spin. These two nuclides have the highest  $Q_{\beta\beta}$  values: 4.272 MeV for  $^{48}\text{Ca}$  and 3.350 MeV for  $^{96}\text{Zr}$ . Only two other “conventional” candidates have  $Q_{\beta\beta}$  greater than 3 MeV:  $^{100}\text{Mo}$  (3.034 MeV) and  $^{150}\text{Nd}$  (3.368 MeV) [20].

<sup>2</sup>Thus, “unconventional” schemes highly increase the list of potentially  $2\beta$  decaying nuclides for studies.

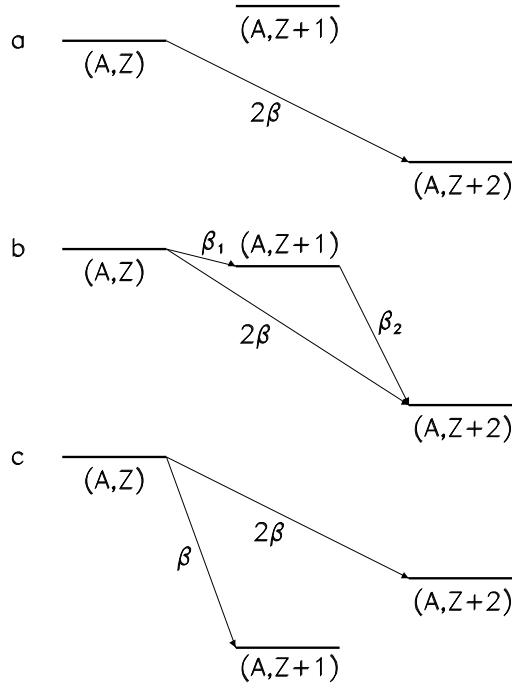


Figure 1: Different configurations of  $(A, Z) - (A, Z + 1) - (A, Z + 2)$  nuclei: (a) “conventional”  $2\beta^-$  triplet when mass of intermediate nuclide  $(A, Z + 1)$  is larger than that of initial  $(A, Z)$  and final  $(A, Z + 2)$  nuclei, and thus ordinary  $\beta^-$  decay of  $(A, Z)$  is forbidden; (b) and (c) “unconventional” configurations when  $2\beta$  decay is one of the branches of  $(A, Z)$  decay. The similar picture can be drawn also for  $2\beta^+$  decay.

been proposed till now. Nevertheless, two more or less realistic methods could be suggested for these investigations.

(1) Use of artificial unstable nuclides produced with accelerators or reactors<sup>3</sup>, which then will be used for  $2\beta$  decay quest. Current possibilities to create radioactive ion beams on accelerators and accumulate them in storage rings are on the level of  $10^{19}$  nuclei per year [21]. As concerning the reactor-produced isotopes, such an approach was already employed once in radiochemical search for  $2\beta$  decay of  $^{244}\text{Pu}$  where the limit (on all modes) was set as  $T_{1/2} \geq 1.1 \times 10^{18}$  yr [22].

(2) Use of appropriate unstable nuclides in natural radioactive U/Th families. These chains are present in some quantities, as contamination, in any materials including those used for low background detectors. Thus, limits on  $2\beta$  decays of such “unconventional” isotopes can be derived as by-product of any low background measurements with the proper detector (including searches for “conventional”  $2\beta$  decay). Moreover, detectors specially loaded by these radioactive isotopes could be produced for such experiments in order to increase the number of nuclei for investigation.

Further, we would like to concentrate on the second possibility and present the experimental results, which were obtained by using this method for the first time.

<sup>3</sup>Besides, such nuclides (but in much less quantities) could be produced in detector by cosmic rays. Nucleon- and muon-induced reactions in a target with given  $(A, Z)$  could result in creation of many different radioactive nuclei with lower  $A$  and  $Z$  numbers.

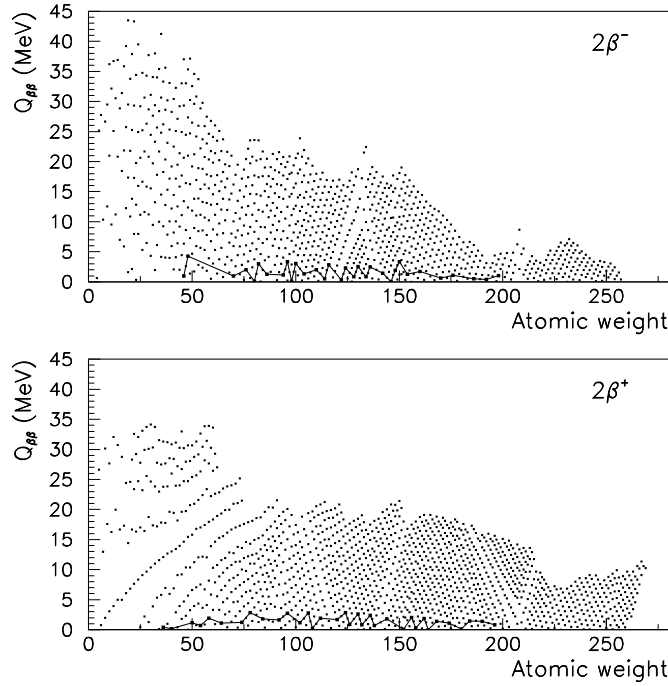


Figure 2: Energy release in double beta decay. The  $Q_{\beta\beta}$  values were extracted from [20]. For “conventional”  $2\beta$  decaying nuclides, points are shown in bold and connected by line.

In order to make a choice of a right candidate for study, let us consider an experimental sensitivity of the mentioned approach. For radioactive chain in equilibrium, decay rates of different isotopes,  $R^{\alpha/\beta} = dN/dt$ , are the same. One can determine the number of nuclei  $N$  for each isotope by using the relation  $N = R^{\alpha/\beta} \cdot T_{1/2}^{\alpha/\beta} / \ln 2$ . Here a small contribution from  $2\beta$  decay is neglected;  $T_{1/2}^{\alpha/\beta}$  is the isotope’s half-life for the usual  $\alpha$  or  $\beta$  decay. From the other side, the limit on half-life for  $2\beta$  decay is equal  $\lim T_{1/2}^{2\beta} = \varepsilon \cdot \ln 2 \cdot N \cdot t / \lim S$ , where  $\varepsilon$  is the efficiency to detect the  $2\beta$  process,  $t$  is the time of measurements, and  $\lim S$  is the limit on the number of observed  $2\beta$  events which can be excluded with a given confidence level on the basis of experimental data. Combining these two equations and expressing the  $\alpha/\beta$  decay rate  $R^{\alpha/\beta}$  through the observed specific activity  $A^{\alpha/\beta} = R^{\alpha/\beta} / m$  ( $m$  is the mass of detector), one can get finally:

$$\lim T_{1/2}^{2\beta} = \varepsilon \cdot m \cdot t \cdot A^{\alpha/\beta} \cdot T_{1/2}^{\alpha/\beta} / \lim S. \quad (1)$$

From the latter one can see immediately that the larger is  $T_{1/2}^{\alpha/\beta}$  half-life of candidate nuclide, the higher  $T_{1/2}^{2\beta}$  limit could be established. To obtain non-trivial bound  $\lim T_{1/2}^{2\beta} > T_{1/2}^{\alpha/\beta}$ , the condition  $\varepsilon \cdot m \cdot t \cdot A^{\alpha/\beta} / \lim S > 1$  should be fulfilled. For typical values of  $\varepsilon \approx 1$  (if  $2\beta$  decaying isotope is containing in the detector itself), one year of measurements,  $\lim S = 2.4$  counts (i.e., for zero observed  $2\beta$  events [23]),  $m = 1$  kg, and  $A^{\alpha/\beta} = 1 \mu\text{Bq/kg}$  (so, for quite low contamination of detector by U/Th chains), we obtain the ratio  $\lim T_{1/2}^{2\beta} / T_{1/2}^{\alpha/\beta} \approx 10$ . For the higher level of contamination  $A^{\alpha/\beta} = 1 \text{ mBq/kg}$ , this ratio is equal  $10^4$ .

In conclusion, to reach the higher sensitivity one has to select the candidate nuclides with the largest  $Q_{\beta\beta}$  energies and with the longest  $T_{1/2}^{\alpha/\beta}$  values. In Table 1, where the properties of all potentially  $2\beta$  decaying nuclei in U/Th families are summarized, there are 11 double  $\beta$  unstable nuclides in the  $^{232}\text{Th}$  chain, 6 nuclides in the  $^{235}\text{U}$  chain, and 16 ones in the  $^{238}\text{U}$  chain [24]. Unfortunately, most of these candidates are out of our interest because of their small  $Q_{\beta\beta}$  energies, short  $T_{1/2}^{\alpha/\beta}$  half-lives, or because of tiny branching ratios in the chain,  $\lambda$ . For example,  $^{210}\text{Tl}$  has one of the highest  $Q_{\beta\beta}$  value 5.548 MeV, but its half-life is too short ( $T_{1/2}^{\beta} = 1.30$  m) and branching ratio is very low ( $\lambda = 0.021\%$ ).

In the present work we report the first experimental results of the quest for  $2\beta$  decays of unstable nuclides in U/Th chains performed in the real-time measurements with the low-background  $\text{CaWO}_4$ ,  $\text{CdWO}_4$  and  $\text{Gd}_2\text{SiO}_5$  crystal scintillators, which contain these nuclides as trace contaminations.

## 2 Experiments and data analysis

The experiments were carried out in the Solotvina Underground Laboratory of INR in a salt mine 430 m underground ( $\simeq 1000$  mwe, with a cosmic muon flux of  $1.7 \times 10^{-6} \text{ cm}^{-2} \text{ s}^{-1}$ , a neutron flux  $\leq 2.7 \times 10^{-6} \text{ cm}^{-2} \text{ s}^{-1}$ , and a radon concentration in the air  $< 30 \text{ Bq m}^{-3}$ ) [26]. The total exposure was equal 1734 h with  $\text{CaWO}_4$  (13316 h with  $\text{CdWO}_4$  and 13949 h with  $\text{Gd}_2\text{SiO}_5$ ) detector.

Since detailed descriptions of the apparatus and technique of the experiments with  $\text{CdWO}_4$  and  $\text{Gd}_2\text{SiO}_5$  detectors are given in refs. [12, 15, 11], below we will describe only the main features, performances and experimental procedure used with the  $\text{CaWO}_4$  crystal scintillator [27].

The  $\text{CaWO}_4$  crystal used has dimensions  $40 \times 34 \times 23$  mm (mass of 189 g). Its measured light output (peak emission at 440 nm with decay time of  $\approx 9 \mu\text{s}$ ) is  $\approx 19\%$  as compared with that of  $\text{NaI}(\text{Tl})$ . The crystal was viewed by the special low-radioactive 5'' photomultiplier tube (EMI D724KFLB) through the quartz light-guide  $\varnothing 10 \times 33$  cm. The detector was surrounded by a passive shield made of teflon (thickness of 3–5 cm), plexiglass (6–13 cm), high purity copper (3–6 cm), lead (15 cm) and polyethylene (8 cm). Two plastic scintillators ( $120 \times 130 \times 3$  cm) installed above the passive shield were used as a cosmic muons veto. Event-by-event data acquisition (the same used with  $\text{CaWO}_4$ ,  $\text{CdWO}_4$  and  $\text{Gd}_2\text{SiO}_5$  detectors) records information on the amplitude (energy), arrival time and pulse shape of a signal (for  $\text{Gd}_2\text{SiO}_5$  pulse shape data were not recorded). For the latter, a transient digitizer based on the fast 12 bit ADC was used with the sample frequency of 20 MS/s [28]. Events in the chosen energy interval (for the  $\text{CaWO}_4$  usually with the energies higher than  $\approx 180$  keV) were recorded in 2048 channels with 50 ns channel's width. The linearity of the energy scale and resolution of the detector were measured with  $^{60}\text{Co}$ ,  $^{137}\text{Cs}$ ,  $^{207}\text{Bi}$ ,  $^{232}\text{Th}$  and  $^{241}\text{Am}$   $\gamma$  sources in the energy range of 60–2615 keV. For example, FWHM is equal 9.7% at the energy 662 keV. The  $\alpha/\beta$  ratio<sup>4</sup> of the crystal was measured with the help of collimated  $\alpha$  particles ( $^{241}\text{Am}$ ) in the range of 0.5–5.3 MeV by using the set of thin mylar films (see for details [29]). Besides,  $\alpha$  peaks of  $^{147}\text{Sm}$  and nuclides from the  $^{232}\text{Th}$ ,  $^{235}\text{U}$  and  $^{238}\text{U}$  families, present as trace in the  $\text{CaWO}_4$  crystal, were used to extend the energy interval up to  $\simeq 8$  MeV. Alpha peaks of  $^{147}\text{Sm}$ ,  $^{210}\text{Po}$ ,  $^{218}\text{Po}$ ,

---

<sup>4</sup>The  $\alpha/\beta$  ratio is defined as ratio of  $\alpha$  peak position in the energy scale measured with  $\gamma$  sources to the energy of  $\alpha$  particles.

Table 1: List of candidate nuclides (present in U/Th radioactive chains), which could undergo  $2\beta^-$  decay, and half-life limits,  $T_{1/2}^{2\beta}$ , determined in this work. The branching ratios,  $\lambda$ , for each nuclide in chain are taken from [24]. Only for  $^{238}\text{U}$  the half-life for  $2\beta$  decay (all modes) was previously measured in radiochemical experiment as  $T_{1/2}^{2\beta} = (2.0 \pm 0.6) \times 10^{21}$  yr [25].

Parent nuclide	Main channel of decay and $T_{1/2}^{\alpha/\beta}$	$\lambda$ , %	$Q_{\beta\beta}$ , MeV	$\lim T_{1/2}^{2\beta}$ at 68% C.L. for $0\nu$ ( $2\nu$ ) mode	
$^{232}\text{Th}$ chain					
$^{232}_{90}\text{Th}$	$\alpha$	$1.405 \times 10^{10}$ yr	100	0.842	$1.6 \times 10^{11}$ ( $2.1 \times 10^9$ ) yr <sup>*)</sup>
$^{228}_{88}\text{Ra}$	$\beta^-$	5.75 yr	100	2.173	–
$^{228}_{89}\text{Ac}$	$\beta^- + \alpha$	6.15 h	100	0.016	–
$^{224}_{87}\text{Fr}$	$\beta^-$	3.30 m	$5.5 \times 10^{-6}$	1.417	–
$^{220}_{86}\text{Rn}$	$\alpha$	55.6 s	100	0.344	–
$^{216}_{84}\text{Po}$	$\alpha$	0.145 s	100	1.534	–
$^{212}_{82}\text{Pb}$	$\beta^-$	10.64 h	100	2.828	6.7 (0.4) yr <sup>**)</sup>
$^{212}_{83}\text{Bi}$	$\beta^- + \alpha$	60.55 m	100	0.500	–
$^{210}_{82}\text{Pb}$	$\beta^- + \alpha$	22.3 yr	$4.3 \times 10^{-9}$	1.226	–
$^{208}_{81}\text{Tl}$	$\beta^-$	3.053 m	35.94	2.121	–
$^{206}_{80}\text{Hg}$	$\beta^-$	8.15 m	$8.2 \times 10^{-17}$	2.841	–
$^{235}\text{U}$ chain					
$^{231}_{90}\text{Th}$	$\beta^-$	25.52 h	100	0.030	–
$^{223}_{87}\text{Fr}$	$\beta^- + \alpha$	21.8 m	1.380	0.563	–
$^{219}_{85}\text{At}$	$\alpha + \beta^-$	56 s	$8.3 \times 10^{-5}$	1.918	–
$^{215}_{83}\text{Bi}$	$\beta^-$	7.6 m	$8.0 \times 10^{-5}$	2.971	–
$^{215}_{84}\text{Po}$	$\alpha + \beta^-$	1.781 ms	100	0.639	–
$^{211}_{82}\text{Pb}$	$\beta^-$	36.1 m	99.99977	1.952	1.5 (0.07) d
$^{238}\text{U}$ chain					
$^{238}_{92}\text{U}$	$\alpha$	$4.468 \times 10^9$ yr	100	1.147	$1.0 \times 10^{12}$ ( $8.1 \times 10^{10}$ ) yr
$^{234}_{90}\text{Th}$	$\beta^-$	24.10 d	100	2.470	144 (2.5) yr
$^{234}_{91}\text{Pa}$	$\beta^-$	6.70 h	100	0.387	17 (0.9) yr
$^{226}_{88}\text{Ra}$	$\alpha + {}^{14}_6\text{C}$	1600 yr	100	0.476	$4.1 \times 10^4$ ( $4.5 \times 10^3$ ) yr
$^{222}_{86}\text{Rn}$	$\alpha$	3.8235 d	100	2.057	2.8 (0.11) yr
$^{218}_{84}\text{Po}$	$\alpha + \beta^-$	3.10 m	100	3.147	3.7 (0.5) d
$^{218}_{85}\text{At}$	$\alpha + \beta^-$	1.6 s	0.020	1.041	–
$^{214}_{82}\text{Pb}$	$\beta^-$	26.8 m	99.980	4.295	87 (1.5) d
$^{214}_{83}\text{Bi}$	$\beta^- + \alpha$	19.9 m	100	2.182	29 (3.5) d
$^{212}_{82}\text{Pb}$	$\beta^-$	10.64 h	$3.2 \times 10^{-9}$	2.828	–
$^{212}_{83}\text{Bi}$	$\beta^- + \alpha$	60.55 m	$3.2 \times 10^{-9}$	0.500	–
$^{210}_{81}\text{Tl}$	$\beta^-$	1.30 m	0.021	5.548	–
$^{210}_{82}\text{Pb}$	$\beta^- + \alpha$	22.3 yr	100	1.226	$1.2 \times 10^5$ ( $8.6 \times 10^3$ ) yr
$^{208}_{81}\text{Tl}$	$\beta^-$	3.053 m	$1.2 \times 10^{-9}$	2.121	–
$^{206}_{80}\text{Hg}$	$\beta^-$	8.15 m	$5.6 \times 10^{-11}$	2.841	–
$^{210}_{80}\text{Ne}$	$\beta^-$	3.38 m	$5.6 \times 10^{-11}$	7.986	–

\*) The limit was set with the  $^{116}\text{CdWO}_4$  (\*\*) – with the  $\text{Gd}_2\text{SiO}_5$ ) detector.

$^{232}\text{Th}$ ,  $^{238}\text{U}$  were selected with the help of a pulse-shape analysis (see below), while  $^{214}\text{Po}$ ,  $^{215}\text{Po}$ ,  $^{216}\text{Po}$ ,  $^{219}\text{Rn}$  and  $^{220}\text{Rn}$  peaks were reconstructed with the help of a time-amplitude analysis from the data accumulated in the low-background measurements. All results (with external and internal  $\alpha$  sources) are in a good agreement. In the energy interval 0.5–2 MeV the  $\alpha/\beta$  ratio decreases with energy:  $\alpha/\beta=0.21(3)-0.020(15)E_\alpha$ , while it increases in the interval of 2–5 MeV:  $\alpha/\beta=0.129(12)+0.021(3)E_\alpha$ , where  $E_\alpha$  is in MeV.

**Pulse-shape discrimination.** The pulse shape of  $\text{CaWO}_4$  scintillation signals can be described by formula:  $f(t) = \sum A_i/(\tau_i - \tau_0) \times (e^{-t/\tau_i} - e^{-t/\tau_0})$ ,  $t > 0$ , where  $A_i$  are amplitudes (in %) and  $\tau_i$  are decay constants for different light emission components,  $\tau_0$  is integration constant of electronics ( $\approx 0.2 \mu\text{s}$ ). The following values were obtained by fitting the average of a large number of individual pulses:  $A_1^\alpha=84\%$ ,  $\tau_1^\alpha = 9.1 \mu\text{s}$ ,  $A_2^\alpha=16\%$ ,  $\tau_2^\alpha = 2.5 \mu\text{s}$  for  $\approx 4.6$  MeV  $\alpha$  particles and  $A_1^\gamma=92\%$ ,  $\tau_1^\gamma=9.2 \mu\text{s}$ ,  $A_2^\gamma=8\%$ ,  $\tau_2^\gamma=2.6 \mu\text{s}$  for  $\approx 1$  MeV  $\gamma$  quanta. This difference allows one to discriminate  $\gamma(\beta)$  events from those of  $\alpha$  particles. For this purpose we used the method of the optimal digital filter (for the first time proposed in [30]), which previously was successfully applied with  $\text{CdWO}_4$  scintillators [28]. To obtain the numerical characteristic of  $\text{CaWO}_4$  signal, so called shape indicator ( $SI$ ), each experimental pulse  $f(t)$  was processed with the following digital filter:  $SI = \sum f(t_k) \times P(t_k) / \sum f(t_k)$ , where the sum is over time channels  $k$ , starting from the origin of pulse and up to  $75 \mu\text{s}$ ,  $f(t_k)$  is the digitized amplitude (at the time  $t_k$ ) of a given signal. The weight function  $P(t)$  is defined as:  $P(t) = \{\bar{f}_\alpha(t) - \bar{f}_\gamma(t)\} / \{\bar{f}_\alpha(t) + \bar{f}_\gamma(t)\}$ , where  $\bar{f}_\alpha(t)$  and  $\bar{f}_\gamma(t)$  are the reference pulse shapes for  $\alpha$  particles and  $\gamma$  quanta, resulting from the average of a large number of experimental pulse shapes.

Shape indicator  $SI$  measured by the  $\text{CaWO}_4$  crystal ( $40 \times 34 \times 23$  mm) for alpha particles in the 1–5.3 MeV region does not depend on the direction of  $\alpha$  irradiation relative to the crystal axes. Similarly, no dependence of the  $SI$  on  $\gamma$  quanta energy (within the energy range 0.1–2.6 MeV) was observed. The distributions of the shape indicator measured with  $\alpha$  particles ( $E_\alpha \approx 4.6$  MeV) and  $\gamma$  quanta ( $\approx 1$  MeV) are depicted in the inset of Fig. 3 (the larger value of the shape indicator corresponds to the shorter decay time of scintillation pulse). As it is seen, distinct discrimination between  $\alpha$  particles and  $\gamma$  rays ( $\beta$  particles) was achieved. An illustration of the PS analysis of the background data, accumulated during 171 h with  $\text{CaWO}_4$  detector, is shown in Fig. 3 as scatter plot for the  $SI$  values versus energy. In this plot one can see two clearly separated populations: the  $\alpha$  events, which belong to U/Th families, and  $\gamma(\beta)$  events.

**Background and radioactive contamination of the  $\text{CaWO}_4$  crystal.** As it is mentioned earlier, the  $\text{CaWO}_4$  crystal ( $40 \times 34 \times 23$  mm) was measured with the help of the low background set-up, installed in the Solotvina Underground Laboratory. The energy resolution of the detector was determined with several  $\gamma$  sources ( $^{60}\text{Co}$ ,  $^{137}\text{Cs}$ ,  $^{207}\text{Bi}$ ,  $^{232}\text{Th}$  and  $^{241}\text{Am}$ ) and can be fitted by function:  $\text{FWHM}_\gamma(\text{keV}) = -3 + \sqrt{6.9E_\gamma}$ , where  $E_\gamma$  is energy of  $\gamma$  quanta in keV. The routine calibrations were carried out weekly with  $^{207}\text{Bi}$  and  $^{232}\text{Th}$  sources.

The energy spectrum of the  $\text{CaWO}_4$  detector, measured during 1734 h in the low background apparatus was separated into  $\alpha$  and  $\beta$  spectra with the help of the pulse-shape discrimination technique.

First, the  $\alpha$  spectrum, which is depicted in Fig. 4, has been analyzed. The intensive and clear peak at the energy 1.28 MeV (in  $\gamma$  scale) can be attributed to intrinsic  $^{210}\text{Po}$  (daughter of  $^{210}\text{Pb}$  from  $^{238}\text{U}$  family) with activity of 0.291(5) Bq/kg. Apparently, the equilibrium of the uranium family in the crystal was broken during crystal production, because peak of  $^{238}\text{U}$

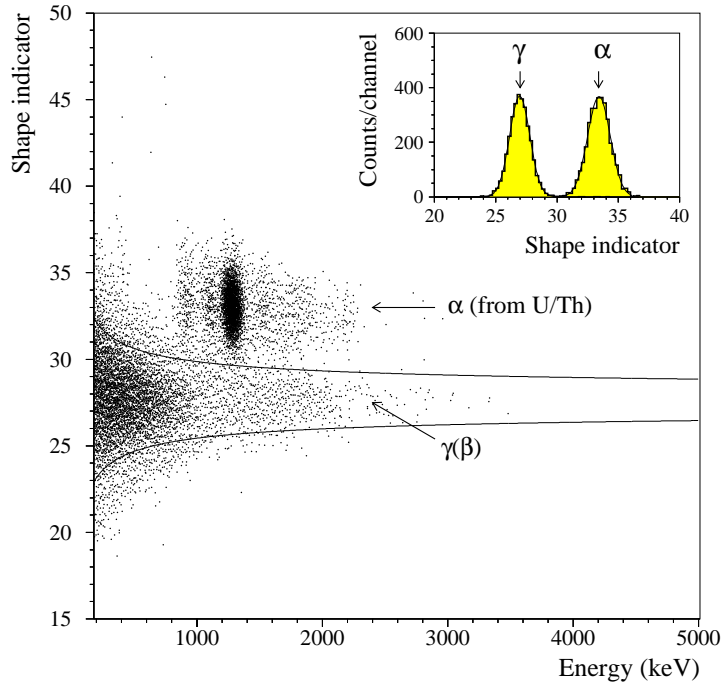


Figure 3: Scatter plot of the shape indicator  $SI$  versus energy for 171 h background data measured with the  $\text{CaWO}_4$  crystal scintillator ( $40 \times 34 \times 23$  mm). Lines show  $\pm 2\sigma$  region of  $SI$  for  $\gamma$  ( $\beta$ ) events. (Inset) The  $SI$  distributions measured in calibration runs with  $\alpha$  particles ( $E_\alpha = 4.6$  MeV which corresponds to  $\approx 1$  MeV in  $\gamma$  scale) and  $\gamma$  quanta ( $\approx 1$  MeV).

(see Inset (a) in Fig. 4) corresponds to the much lower activity of 14.0(5) mBq/kg. Peaks of the uranium's daughters  $^{234}\text{U}$ ,  $^{230}\text{Th}$ ,  $^{226}\text{Ra}$  are not resolved (their  $Q_\alpha$  values are very close), however, the area of the total peak (at  $\approx 1.1$  MeV) is in satisfactory agreement with the activity of  $^{238}\text{U}$  and  $^{226}\text{Ra}$  (see below the results of time-amplitude analysis for  $^{226}\text{Ra}$ ). Another member of the family,  $^{222}\text{Rn}$ , is not discriminated from  $^{210}\text{Po}$  (an expected energy of  $\alpha$  peak is  $\approx 1.34$  MeV in  $\gamma$  scale), while  $^{218}\text{Po}$  is well resolved.

In the low energy part of alpha spectrum (Inset (b) in Fig. 4) the peak at the energy  $\approx 0.8$  MeV can be attributed to  $^{232}\text{Th}$  with activity 0.69(10) mBq/kg. Weak alpha peak with the energy in  $\gamma$  scale of 395(2) keV (corresponds to energy of  $\alpha$  particles 2243(9) keV) can be explained by trace of  $^{147}\text{Sm}$  ( $E_\alpha = 2247$  keV,  $T_{1/2} = 1.06 \times 10^{11}$  yr, isotopic abundance is 15.0% [31]) with activity 0.49(4) mBq/kg. The total internal alpha activity in the calcium tungstate crystal is  $\approx 0.4$  Bq/kg.

Besides, the raw background data were analyzed by the time-amplitude method, when the energy and arrival time of each event were used for selection of some decay chains in  $^{232}\text{Th}$ ,  $^{235}\text{U}$  and  $^{238}\text{U}$  families. For instance, the following sequence of  $\alpha$  decays from the  $^{232}\text{Th}$  family was searched for and observed:  $^{220}\text{Rn}$  ( $Q_\alpha = 6.40$  MeV,  $T_{1/2} = 55.6$  s)  $\rightarrow$   $^{216}\text{Po}$  ( $Q_\alpha = 6.91$  MeV,  $T_{1/2} = 0.145$  s)  $\rightarrow$   $^{212}\text{Pb}$  (which are in equilibrium with  $^{228}\text{Th}$ ). Because the energy of  $\alpha$  particles from  $^{220}\text{Rn}$  decay corresponds to  $\approx 1.6$  MeV in  $\gamma$  scale of  $\text{CaWO}_4$  detector, the events in the energy region 1.4 – 2.2 MeV were used as triggers. Then all events (within 1.4 – 2.2 MeV) following the triggers in the time interval 20 – 600 ms (containing 85.2% of  $^{216}\text{Po}$  decays)



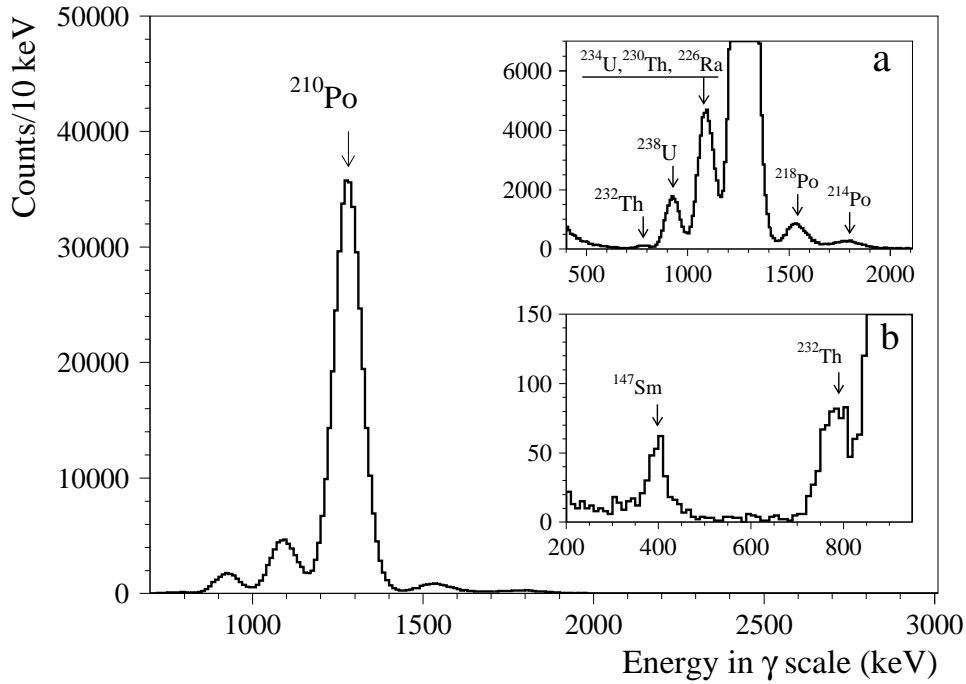


Figure 4: Energy spectrum of  $\alpha$  events selected by the pulse-shape analysis from background data measured with the  $\text{CaWO}_4$  detector (0.189 kg, 1734 h). (Inset a) The same spectrum but scaled up. It is well reproduced by the model, which includes  $\alpha$  decays of nuclides from  $^{232}\text{Th}$  and  $^{238}\text{U}$  families. (Inset b) Low energy part of the  $\alpha$  spectrum.

were selected. The obtained  $\alpha$  peaks (the  $\alpha$  nature of events was confirmed by the pulse-shape analysis described above), as well as the distributions of the time intervals between events are in a good agreement with those expected for  $\alpha$  particles of  $^{220}\text{Rn} \rightarrow ^{216}\text{Po} \rightarrow ^{212}\text{Pb}$  chain<sup>5</sup> (see Fig. 5). On this basis the activity of  $^{228}\text{Th}$  in the  $\text{CaWO}_4$  crystal was calculated as 0.6(2) mBq/kg, which is in a good agreement with activity of  $^{232}\text{Th}$  determined from  $\alpha$  spectrum – 0.69(10) mBq/kg.

For the analysis of the  $^{226}\text{Ra}$  chain ( $^{238}\text{U}$  family) the following sequence of  $\beta$  and  $\alpha$  decays was used:  $^{214}\text{Bi}$  ( $Q_\beta = 3.27$  MeV)  $\rightarrow$   $^{214}\text{Po}$  ( $Q_\alpha = 7.83$  MeV,  $T_{1/2} = 164$   $\mu\text{s}$ )  $\rightarrow$   $^{210}\text{Pb}$ . For the first event the lower energy threshold was set at 0.18 MeV, while for the second decay the energy window 1.6 – 2.4 MeV was chosen. Time interval of 90 – 500  $\mu\text{s}$  (56.3% of  $^{214}\text{Po}$  decays) was used. The obtained spectra for  $^{214}\text{Bi}$  and  $^{214}\text{Po}$  lead to the  $^{226}\text{Ra}$  activity in the  $\text{CaWO}_4$  crystal equal to 5.6(5) mBq/kg.

Finally, let us analyze the energy spectrum of  $\beta(\gamma)$  events selected with the help of the pulse-shape technique and presented in Fig. 6. The counting rate for the  $\beta(\gamma)$  spectrum above the energy threshold of 0.2 MeV is  $\approx 0.45$  counts/(s·kg). The contribution of the external  $\gamma$  rays to this background rate was estimated as small as  $\approx 2\%$ , by using results of measurements with  $\text{CdWO}_4$  crystal (mass of 0.448 kg) installed in the same low background set-up. Therefore, the remaining  $\beta(\gamma)$  events are caused by the intrinsic contaminations of the  $\text{CaWO}_4$  crystal. Major

<sup>5</sup>The  $\alpha$  peak with the energy  $E_\alpha \approx 7.3$  MeV, which is present in the energy distribution of the second event, can be attributed to  $^{215}\text{Po}$  from  $^{235}\text{U}$  family. Corresponding activity of  $^{227}\text{Ac}$  in the crystal is 1.6(3) mBq/kg.

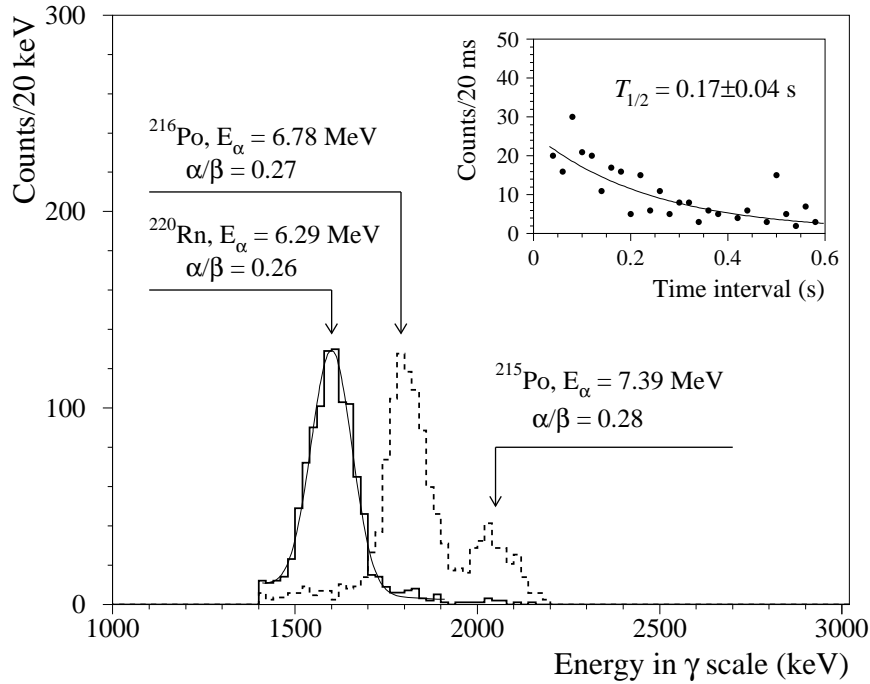


Figure 5: Alpha peaks of  $^{220}\text{Rn}$  and  $^{216}\text{Po}$  selected by the time-amplitude analysis from the data accumulated with the  $\text{CaWO}_4$  detector. (Inset) The distribution of the time intervals between the first and second events (dots) together with the exponential fit (line). Obtained half-life of  $^{216}\text{Po}$  ( $0.17 \pm 0.04$  s) is in an agreement with the table value:  $0.145(2)$  s [24].

part of this  $\beta$  activity can be ascribed to:  $^{210}\text{Bi}$  (daughter of  $^{210}\text{Pb}$ ) – 0.291 Bq/kg;  $^{234m}\text{Pa}$  – 0.014 Bq/kg;  $^{214}\text{Pb}$  and  $^{214}\text{Bi}$  ( $^{238}\text{U}$  family) –  $\approx 0.007$  Bq/kg;  $^{211}\text{Pb}$  ( $^{235}\text{U}$  family) –  $\approx 0.002$  Bq/kg. The remaining  $\beta$  events can be explained by other  $\beta$  active impurities ( $^{40}\text{K}$ ,  $^{90}\text{Sr}$  in equilibrium with  $^{90}\text{Y}$ ,  $^{137}\text{Cs}$ , etc.) probably present in the crystal.

The summary of the measured radioactive contamination of the  $\text{CaWO}_4$ ,  $\text{CdWO}_4$  and  $\text{Gd}_2\text{SiO}_5$  crystal scintillators (or limits on their activities) is given in Table 2 [11, 15, 27]. One can see that radioactive impurities in the  $\text{CaWO}_4$  and  $\text{Gd}_2\text{SiO}_5$  crystals (available at present) are much higher (by factor of  $10 - 10^3$ ) than those of the  $\text{CdWO}_4$  scintillators.

### 3 Limits on $2\beta$ decay and conclusions

The background spectra of  $\beta/\gamma$  events selected by the pulse-shape discrimination method with the  $\text{CaWO}_4$ ,  $\text{CdWO}_4$  and  $\text{Gd}_2\text{SiO}_5$  crystal scintillators were analyzed to search for  $2\beta$  decays of unstable isotopes in U/Th chains. In general, we did not find any peculiarities in the measured spectra which can be attributed to the double beta decay processes searched for. Therefore, only the lower half-life limits were established in accordance with the equation (1).

Values of  $\lim S$  were simply estimated as a square root of the number of counts in the corresponding energy windows of the background spectra. For instance, in the spectrum measured with the  $\text{CaWO}_4$  detector, there are 3937 counts in the energy interval 1110–1200 keV where the peak of the  $0\nu 2\beta$  decay of  $^{238}\text{U}$  is expected. Number of  $^{238}\text{U}$  nuclei is  $N = 5.4 \times 10^{14}$ , and

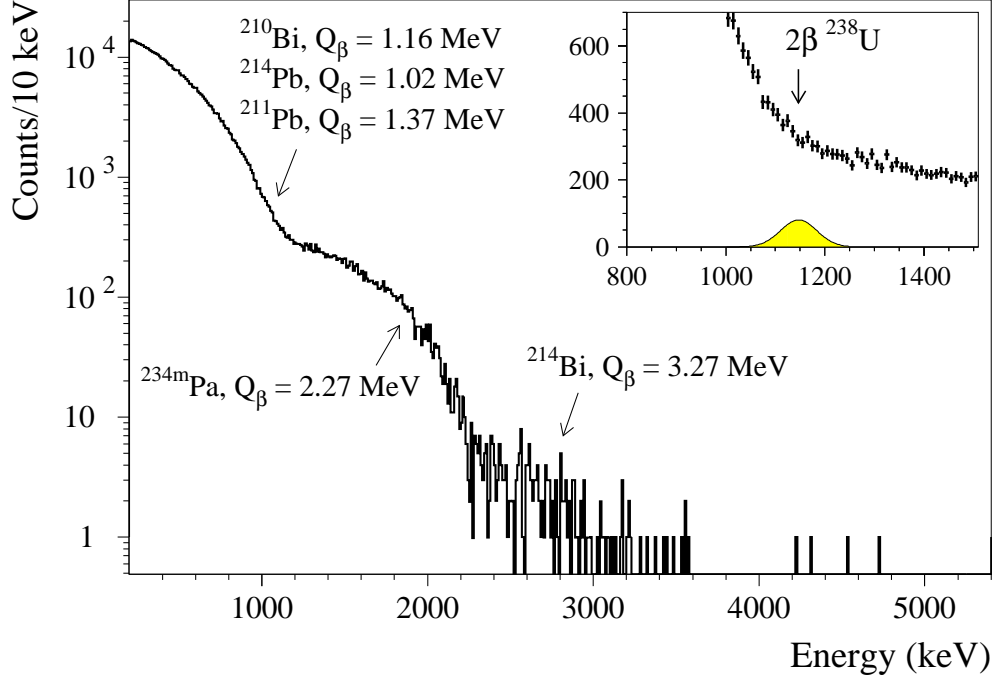


Figure 6: Energy spectrum of  $\beta(\gamma)$  events selected by the pulse-shape analysis from background data measured with the  $\text{CaWO}_4$  detector (0.189 kg, 1734 h). It is described by  $\beta$  spectra of  $^{210}\text{Bi}$  ( $Q_\beta = 1.16$  MeV),  $^{214}\text{Pb}$  ( $Q_\beta = 1.02$  MeV),  $^{211}\text{Pb}$  ( $Q_\beta = 1.37$  MeV),  $^{234m}\text{Pa}$  ( $Q_\beta = 2.27$  MeV), and  $^{214}\text{Bi}$  ( $Q_\beta = 3.27$  MeV). (Inset) The energy region of  $0\nu 2\beta$  decay of  $^{238}\text{U}$  is shown together with expected peak of  $0\nu 2\beta$  decay which corresponds to  $T_{1/2} = 10^{11}$  yr.

efficiency for this energy region is  $\varepsilon = 0.85$ . The  $\text{lim } S = 63$  counts together with the time of measurements  $t = 1734$  h lead to the restriction on the half-life:  $T_{1/2}^{0\nu} \geq 1.0 \times 10^{12}$  yr at 68% C.L.<sup>6</sup> Considering the energy interval 200–760 keV (number of background counts is  $4.7 \times 10^5$ , efficiency  $\varepsilon = 0.75$ ), the half-life limit relatively to the two-neutrino  $2\beta$  decay of  $^{238}\text{U}$  was estimated as:  $T_{1/2}^{2\nu} \geq 8.1 \times 10^{10}$  yr at 68% C.L. In the inset of Fig. 6, the energy spectrum of the  $\text{CaWO}_4$  detector in the region of  $0\nu 2\beta$  decay of  $^{238}\text{U}$  is shown together with the expected peak of  $0\nu 2\beta$  decay ( $T_{1/2} = 10^{11}$  yr).

Similarly, such a procedure was applied to estimate the  $T_{1/2}$  limits for  $2\beta$  decays of other nuclides in U/Th radioactive families in the  $\text{CaWO}_4$  crystal (from Table 1), as well as by using the data accumulated during 13316 h with the  $^{116}\text{CdWO}_4$  detector [12, 15] and with the  $\text{Gd}_2\text{SiO}_5$  scintillator (13949 h) [11]. Pulse-shape and time-amplitude analysis of events were also used to reduce backgrounds. For example, in  $2\beta$  decay of  $^{214}\text{Pb}$  ( $Q_{2\beta} = 4.3$  MeV) the daughter nucleus  $^{214}\text{Po}$  quickly ( $T_{1/2} = 164 \mu\text{s}$ )  $\alpha$  decays with  $Q_\alpha = 7.8$  MeV. Such a chain of two events, first of which (with the energy 4.3 MeV) has the shape of scintillation flash specific for  $\gamma/\beta$  particles, and the second one (7.8 MeV, occurred within  $\approx 1$  ms after the first) has the pulse

<sup>6</sup>Similar results were obtained in more sophisticated approach, when the experimental spectrum was fitted by the sum of background model and response function of the set-ups for  $2\beta$  decay searched for (both were Monte Carlo simulated with the GEANT3.21 and DECAY4 codes [11, 12, 15, 29]). Therefore, notwithstanding its simplicity, the “square root” approach gives a right scale of the sensitivity of an experiment.

Table 2: Radioactive contaminations measured in the  $\text{CaWO}_4$  (mass of 189 g, measuring time 1734 h),  $\text{CdWO}_4$  (330 g, 13316 h) and  $\text{Gd}_2\text{SiO}_5$  (635 g, 13949 h) crystal scintillators.

Chain	Sub-chain	Activity (mBq/kg)		
		$\text{CaWO}_4$	$^{116}\text{CdWO}_4$	$\text{Gd}_2\text{SiO}_5$
$^{232}\text{Th}$	$^{232}\text{Th}$	0.69(10)	0.053(9)	$\leq 6.5$
	$^{228}\text{Ra} \dots ^{228}\text{Ac}$	–	$\leq 0.004$	$\leq 9$
	$^{228}\text{Th} \dots$ end of chain	0.6(2)	0.039(2)	2.287(13)
$^{235}\text{U}$	$^{231}\text{Pa}$	–	–	$\leq 0.08$
	$^{227}\text{Ac} \dots$ end of chain	1.6(3)	0.0014(9)	0.948(9)
$^{238}\text{U}$	$^{238}\text{U} \dots ^{234}\text{Pa}$	14.0(5)	$\leq 0.6$	$\leq 2$
	$^{234}\text{U}$	–	$\leq 0.6$	–
	$^{230}\text{Th}$	–	$\leq 0.5$	$\leq 9$
	$^{226}\text{Ra} \dots ^{214}\text{Po}$	5.6(5)	$\leq 0.004$	0.271(4)
	$^{210}\text{Pb} \dots$ end of chain	291(5)	$\leq 0.4$	$\leq 0.8$

shape character to  $\alpha$ 's, gives a very distinctive signature, which helps to suppress background greatly.

All results of the search for the  $2\beta$  decays of the radioactive nuclides in thorium and uranium families obtained in this work are summarized in Table 1 (only half-life limits are given whose values exceed one day).

In conclusion, we have presented results of the first experimental search (in direct counting experiment) for the  $2\beta$  decays of  $\alpha/\beta$  decaying nuclides in U/Th chains, which are present in the  $\text{CaWO}_4$ ,  $\text{CdWO}_4$  and  $\text{Gd}_2\text{SiO}_5$  crystal scintillators as contaminations. The results were obtained by reanalyzing the data accumulated during few years of measurements in the Solotvina Underground Laboratory with these detectors, whose properties (radioactive contaminations, energy resolutions,  $\alpha/\beta$  ratios and pulse-shapes) were carefully studied.

The half-life limits derived in this first attempt are in the range from a few days to  $10^{12}$  yr, i.e. much more modest than those of “conventional”  $2\beta$  decay experiments. Obviously, the sensitivity of our method could be further enhanced by producing scintillators loaded by thorium or uranium (the level of allowed concentration of these nuclides is restricted by the requirement of reasonable counting rate and by demand to keep satisfactory scintillation characteristics of the detector). For example, supposing the use of some fast scintillator (with decay time in the range of ns), the activity of the U/Th admixture could be increased to  $\simeq 10^4$  Bq/kg in comparison with the current level of  $\sim 1$  mBq/kg. Together with the total mass of detectors enlarged from  $\simeq 0.1$  kg to 100 kg, it could allow one to advance the current limits on  $2\beta$  half-lives of nuclides in U/Th chains by  $\simeq 10$  orders of magnitude, which looks interesting.

Let us consider also the unstable nuclides, which can be produced with accelerators or reactor for the  $2\beta$  decay searches. There exist plans of large-scale experiments with quickly  $\beta$  decaying radioactive ions [21] (producing intensive beams of pure  $\nu_e$  and  $\tilde{\nu}_e$ ) for high precision measurements of neutrino oscillations with the future megaton Frejus detector [34]. These experiments could give, as by-product, some results on  $0\nu 2\beta$  decay of involved nuclei. However, even principal schemes for extraction of such by-products were not debated yet. As an inspiring example, we can mention the experiment [35], where  $\alpha$  active  $^{221}\text{Ra}$  isotope with  $T_{1/2} = 28$  s

was produced by bombarding a thorium target with the 600 MeV proton beam. Then, the cluster radioactivity (emission of  $^{14}\text{C}$ ) of  $^{221}\text{Ra}$  was observed with  $T_{1/2} = 7.8 \times 10^5$  yr [35], that is  $\approx 10^{12}$  times longer than half-life of  $^{221}\text{Ra}$  alpha decay.

Besides, by analyzing the table of isotopes [24] for the long lived unstable nuclei (with  $T_{1/2} > 1$  yr), which can simultaneously undergo  $2\beta$  decay, three nuclides were found with  $Q_{2\beta}$  values higher than 4 MeV:  $^{42}\text{Ar}$  ( $T_{1/2}=32.9$  yr,  $Q_{2\beta}=4125$  keV),  $^{126}\text{Sn}$  ( $T_{1/2}\simeq 1 \times 10^5$  yr,  $Q_{2\beta}=4050$  keV) and  $^{208}\text{Po}$  ( $T_{1/2}=2.9$  yr,  $Q_{2EC}=4280$  keV). From them,  $^{126}\text{Sn}$  seems to be the most interesting due to its longest life-time. As a possible detector for the  $0\nu 2\beta$  decay quest of  $^{126}\text{Sn}$ , the liquid scintillator loaded by  $^{126}\text{Sn}$  (up to  $\simeq 10$ – $20\%$  in mass [36]) could be considered. The contribution of two successive single  $\beta$  decays  $^{126}_{50}\text{Sn}$  ( $T_{1/2} \simeq 1 \times 10^5$  yr,  $Q_{\beta}=380$  keV)  $\rightarrow$   $^{126}_{51}\text{Sb}$  ( $T_{1/2}=12.5$  d,  $Q_{\beta}=3670$  keV)  $\rightarrow$   $^{126}_{52}\text{Te}$  to background in the energy window of the  $0\nu 2\beta$  decay of  $^{126}\text{Sn}$  would be negligible due to the long half-life of the intermediate  $^{126}\text{Sb}$  nucleus and taking into account the energy distributions of both ( $^{126}\text{Sn}$  and  $^{126}\text{Sb}$ )  $\beta$  spectra. We recall that there is only one “convenient”  $2\beta$  candidate with  $Q_{2\beta} > 4$  MeV:  $^{48}\text{Ca}$ , whose natural abundance is very low (0.19%) that results in the world reserve of  $\simeq 50$  g of enriched  $^{48}\text{Ca}$  isotope available for the investigations [9]. Note that for equal experimental  $T_{1/2}$  limits on  $0\nu 2\beta$  decay, an experiment with  $^{126}\text{Sn}$  would be more sensitive to the neutrino mass than that with  $^{48}\text{Ca}$  due to higher phase space available (which depends not only on the  $Q_{2\beta}$  but on the  $Z$  value of a nucleus as well). However, perspectives to obtain considerable amounts of  $^{126}\text{Sn}$  isotope are unclear.

Nevertheless, we believe that in the light of the present day status of the  $2\beta$  decay research<sup>7</sup> it is useful to discuss and test some “unconventional” (unusual and even strange) ideas and approaches to detect the  $0\nu 2\beta$  decay, like ones presented in this paper, even notwithstanding the modest experimental limits reached for the first time and quite uncertain perspectives of their advancement from the to-date point of view.

## References

- [1] Y. Fukuda et al. (Super-Kamiokande Collaboration), Phys. Rev. Lett. 81 (1998) 1562; M. Ambrosio et al. (MACRO Collaboration), Phys. Lett. B 517 (2001) 59; W.W.M. Allison et al. (Soudan-2 Collaboration), Phys. Lett. B 449 (1999) 137.
- [2] S. Fukuda et al. (Super-Kamiokande Collaboration), Phys. Rev. Lett. 86 (2001) 5651; Q.R. Ahmad et al. (SNO Collaboration), Phys. Rev. Lett. 87 (2001) 071301; 89 (2002) 011302; S.N. Ahmed et al. (SNO Collaboration), nucl-ex/0309004.
- [3] K. Eguchi et al. (KamLAND Collaboration), Phys. Rev. Lett. 90 (2003) 021802.
- [4] M.H. Ahn et al., Phys. Rev. Lett. 90 (2003) 041801.
- [5] J.D. Vergados, Phys. Rep. 361 (2002) 1.
- [6] Yu.G. Zdesenko, Rev. Mod. Phys. 74 (2002) 663.
- [7] S.R. Elliot and P. Vogel, Ann. Rev. Nucl. Part. Sci. 52 (2002) 115.

---

<sup>7</sup>In order to make *discovery* of the  $0\nu 2\beta$  decay indeed realistic, the level of experimental sensitivity should be advanced to  $m_{\nu} \approx 0.01$  eV [5, 6, 7], which, however, could be beyond reach of current technologies applied within the framework of “conventional” methods.

- [8] V.I. Tretyak and Yu.G. Zdesenko, *At. Data Nucl. Data Tables* 80 (2002) 83.
- [9] R.K. Bardin et al., *Nucl. Phys. A* 158 (1970) 337;  
V.B. Brudanin et al., *Phys. Lett. B* 495 (2000) 63.
- [10] A.A. Klimenko et al., *Nucl. Instrum. Meth. B* 17 (1986) 445;  
A. De Silva et al., *Phys. Rev. C* 56 (1997) 2451.
- [11] F.A. Danevich et al., *Nucl. Phys. A* 694 (2001) 375.
- [12] F.A. Danevich et al., *Nucl. Phys. A* 717 (2003) 129.
- [13] S.R. Elliot et al., *Phys. Rev. C* 46 (1992) 1535.
- [14] H. Ejiri et al., *Phys. Rev. C* 63 (2001) 065501.
- [15] F.A. Danevich et al., *Phys. Rev. C* 62 (2000) 045501; 68 (2003) 035501.
- [16] C. Arnaboldi et al., *Phys. Lett. B* 557 (2003) 167.
- [17] R. Luescher et al., *Phys. Lett. B* 434 (1998) 407.
- [18] H.V. Klapdor-Kleingrothaus et al., *Eur. Phys. J. A* 12 (2001) 147;  
C.E. Aalseth et al., *Phys. Rev. C* 59 (1999) 2108; *Phys. Rev. D* 65 (2002) 092007.
- [19] J. Suhonen and O. Civitarese, *Phys. Rep.* 300 (1998) 123.
- [20] G. Audi and A.H. Wapstra, *Nucl. Phys. A* 595 (1995) 409.
- [21] P. Zucchelli, *Phys. Lett. B* 532 (2002) 166; talk at NNN'02 Workshop, 16-18.01.2002, CERN, 2002.
- [22] K.J. Moody et al., *Phys. Rev. C* 46 (1992) 2624.
- [23] D.E. Groom et al., *Eur. Phys. J. C* 15 (2000) 1.
- [24] *Table of isotopes*, ed. by R.B. Firestone et al., 8th ed., John Wiley & Sons, New York, 1996 and CD update, 1998.
- [25] A.L. Turkevich et al., *Phys. Rev. Lett.* 67 (1991) 3211.
- [26] Yu.G. Zdesenko et al., *Proc. 2nd Int. Symp. Underground Physics, Baksan Valley, USSR, August 17–19, 1987. – Moscow, Nauka, 1988, p. 291.*
- [27] Yu.G. Zdesenko et al., submitted to *Nucl. Instr. Meth. A*.
- [28] T. Fazzini et al., *Nucl. Instr. Meth. A* 410 (1998) 213.
- [29] F.A. Danevich et al., *Phys. Rev. C* 67 (2003) 014310.
- [30] E. Gatti and F. De Martini, *Nuclear Electronics* 2, IAEA, Vienna, 1962, p. 265.
- [31] K.J.R. Rosman and P.D.P. Taylor, *Pure and Appl. Chem.* 70 (1998) 217.

- [32] GEANT, CERN Program Library Long Write-up W5013, CERN, 1994.
- [33] O.A. Ponkratenko et al., Phys. At. Nucl. 63 (2000) 1282.
- [34] J. Bouchez et al., hep-ex/0310059.
- [35] R. Bonetti et al., Nucl. Phys. A 576 (1994) 21.
- [36] G.F. Knoll, *Radiation Detection and Measurement*, 3rd ed., John Wiley & Sons, New York, 2000.